

Hexcitons and excitons in monolayer WSe₂

Dinh Van Tuan,¹ Su-Fei Shi,^{2,3} Xiaodong Xu,^{4,5} Scott A. Crooker,⁶ and Hanan Dery^{1,7,*}

¹*Department of Electrical and Computer Engineering,
University of Rochester, Rochester, New York 14627, USA*

²*Department of Chemical and Biological Engineering,
Rensselaer Polytechnic Institute, Troy, NY, 12180, USA*

³*Department of Electrical, Computer and Systems Engineering,
Rensselaer Polytechnic Institute, Troy, NY, 12180, USA*

⁴*Department of Physics, University of Washington, Seattle, Washington 98195, USA*

⁵*Department of Materials Science and Engineering,
University of Washington, Seattle, Washington 98195, USA*

⁶*National High Magnetic Field Laboratory, Los Alamos, New Mexico 87545, USA*

⁷*Department of Physics and Astronomy, University of Rochester, Rochester, New York 14627, USA*

In the archetypal monolayer semiconductor WSe₂, the distinct ordering of spin-polarized valleys (low-energy pockets) in the conduction band allows for studies of not only simple neutral excitons and charged excitons (i.e., trions), but also more complex many-body states that are predicted at higher electron densities. We discuss magneto-optical measurements of electron-rich WSe₂ monolayers, and interpret the spectral lines that emerge at high electron doping as optical transitions of 6-body exciton states (“hexcitons”) and 8-body exciton states (“oxcitons”). These many-body states emerge when a photoexcited electron-hole pair interacts simultaneously with multiple Fermi seas, each having distinguishable spin and valley quantum numbers. In addition, we identify the energies of primary and satellite optical transitions of hexcitons in the photoluminescence spectrum.

Hydrogen-like bound states of photoexcited electron-hole pairs in semiconductors – that is, excitons – have been a focus of considerable study for more than half a century [1–5]. In undoped direct-gap semiconductors, neutral excitons comprise the photogenerated electron and hole in the conduction and valence bands (CB and VB), respectively, and typically manifest as discrete optical resonances below the free-particle band-gap energy. More interesting states arise when electron-hole (*e-h*) pairs are photoexcited into doped semiconductors containing a Fermi sea of mobile carriers [4–12]. Most well-known are the charged excitons (or trions) that emerge in lightly electron- or hole-doped semiconductors [13–15]. In the simplest picture, a trion is a three-particle complex consisting of a carrier from the Fermi sea bound to the photoexcited *e-h* pair. Trions appear as an additional optical resonance below the neutral exciton, and the energy difference between the two provides a measure of the binding energy between the exciton and the resident carrier: ~ 1 -5 meV in semiconductors such as GaAs or ZnSe [16–18], and ~ 20 -30 meV in monolayer (ML) semiconductors such as MoS₂ or WSe₂ [19].

A proper microscopic description of charged excitons remains a topic of active debate and long-standing theoretical interest, rejuvenated recently by detailed spectroscopy of charge-tunable transition-metal dichalcogenide MLs [19–25]. For example, drawing on concepts in cold-atom physics [26, 27], it was recently suggested that the optical resonances attributed to trions and excitons can be regarded as the attractive and repulsive branches, respectively, of the collective Fermi-sea response to a photoexcited *e-h* pair [28–31]. An alternative picture, dating back over two decades, considers the ground state as a

four-particle “tetron” complex, wherein the trion moves together and is correlated with the hole in the Fermi sea (the so-called Fermi or CB hole) that is created when the trion forms [32–35]. Relationships between these various pictures have been discussed in recent literature [36–39]. Common to these pictures is that the photoexcited *e-h* pair interacts primarily with resident carriers that are quantum-mechanically distinguishable. The electrons can then stay together near the VB hole without violating the Pauli exclusion principle. In electron-doped semiconductors such as GaAs or MoSe₂, photoexcited electrons belong to one of the two reservoirs populated by resident electrons. As a result, the *e-h* pair primarily interacts with one available reservoir of electrons with distinguishable quantum numbers.

However, entirely new classes of increasingly complex many-body excitons are predicted to emerge if the photoexcited *e-h* pair can interact simultaneously with *multiple* distinguishable electrons [40, 41]. Fortunately, the ordering of the spin-polarized CB valleys at the $\pm K$ points of ML-WSe₂ provides an ideal platform to investigate such novel many-body states. As depicted in Fig. 1(a), the low-energy excitonic transition in this ML couples to the *top* (not bottom) CB valleys at the $\pm K$ points. This leaves the photoexcited *e-h* pair free to interact with both reservoirs of distinguishable electrons in the bottommost CB valleys. In this Letter, we present magneto-optical experiments that provide evidence for 6-particle “hexcitons” and even 8-particle “oxcitons” that emerge when a photoexcited *e-h* pair in doped WSe₂ interacts simultaneously with two or even three reservoirs of distinguishable electrons. Numerical calculations of the hexciton binding energy support this scenario [42].

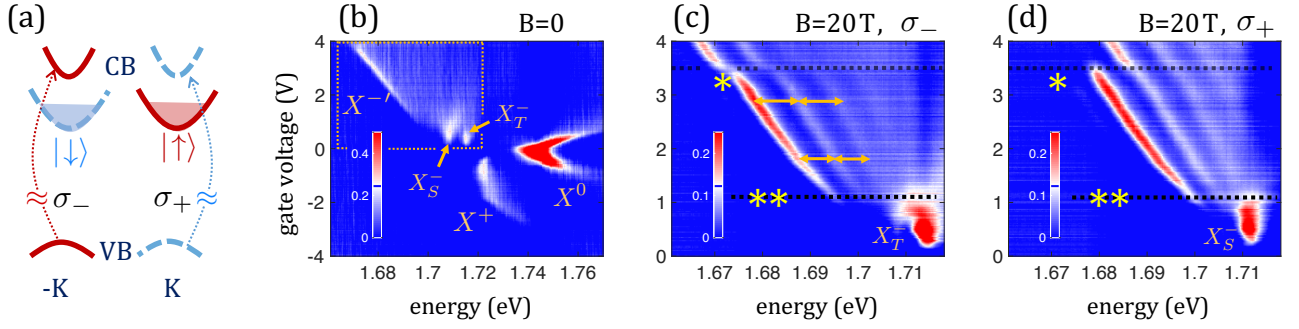


FIG. 1. (a) Helicity resolved optical transitions in ML-WSe₂. Light excitation with σ_+ (σ_-) helicity corresponds to optical transitions at the K ($-K$) valley. Resident electrons occupy the bottommost valleys, whereas photoexcited electrons belong in the top valleys. (b) Optical reflectance spectra at 4 K as a function of gate voltage and photon energy. (c) and (d) Helicity resolved magneto-optical reflectance spectra when the out-of-plane magnetic field is 20 T, shown in the spectral and voltage windows that are marked by the dotted box in (b).

Figure 1(b) shows the density-dependent optical reflectivity spectra from a charge-tunable single ML-WSe₂ at zero magnetic field (see Ref. [22] for sample and experimental details). Essentially, similar behavior has been reported by several groups [20, 24, 25]. When the ML is undoped, only the neutral exciton resonance appears (X^0). Positively- and negatively-charged excitons (X^\pm) emerge at lower energies when the ML is lightly hole- and electron-doped, respectively. Note that *two* distinct X^- resonances appear in WSe₂, because photoexcited e - h pairs can interact with either opposite-spin electrons in the same valley (singlet, X_S^-), or with same-spin electrons in the opposite valley (triplet, X_T^-), forming intravalley and intervalley trions [43, 44].

At higher electron density n_e , the features $X_{S,T}^-$ disappear and a strong new resonance, often called X'^- , emerges at even lower energy and redshifts further with increasing n_e . Its origin is not understood, despite having been first observed in 2013 [45]. That a similar resonance never appears on the hole-doped side is already a compelling argument that X'^- is not related to simple exciton-polarons, tetrons, or transitions between free electron-hole pairs. We argue below that X'^- corresponds to the stable formation of a 6-body hexciton state, which forms in ML-WSe₂ when a photoexcited e - h pair interacts simultaneously with electrons from the bottommost CB valleys at K and $-K$.

We focus on the emergence and evolution of the optical transition with charge density in applied magnetic fields B . The field breaks the valley degeneracy, thereby allowing us to better control the population in each of the four spin-polarized CB valleys. Figures 1(c) and (d) show density-dependent maps of the σ^\pm circular-polarized optical reflectivity at $B=20$ T. At this large field, the resonance splits to a series of lines that are reminiscent of Landau level (LL) formation.

A first piece of evidence favoring hexciton formation is that the LLs appear *simultaneously* in both σ^\pm polar-

izations when $V_g \approx 1$ V (corresponding to $n_e \sim 1 - 2 \times 10^{12} \text{ cm}^{-2}$). At smaller densities, free electrons fill only the spin-up CB valley at K , whose energy is shifted down by the magnetic field. Consequently, the spectrum only includes the resonances X_S^- with σ_+ polarization and X_T^- with σ_- polarization. At voltages larger than ~ 1 V, indicated by dotted lines with two asterisks in Figs. 1(c) and (d), the Fermi sea begins to fill the spin-down CB valley at $-K$. This threshold provides two distinguishable reservoirs of free electrons with which a photoexcited e - h pair can simultaneously interact, forming the 6-particle hexciton (depicted in Figs. 3(b) and (c)).

A second noteworthy feature occurs at larger electron densities, when $V_g \approx 3.5$ V, indicated by dotted lines with one asterisk in Figs. 1(c) and (d). The lowest energy resonance with σ^+ polarization abruptly disappears, indicating that the Fermi sea has just filled the lowest LL in the top CB valley at K , which quenches the corresponding optical transition due to Pauli blocking. More importantly, concurrent with the quenching in σ_+ , the optical resonances in σ_- exhibit a discontinuous redshift. Namely, the binding energy of the complex in $-K$ abruptly *increases* (by $\sim 3\text{meV}$) when free electrons fill not only the two bottommost CB valleys but also a third CB valley having distinguishable quantum numbers (spin-down in K). This threshold marks the transition from hexcitons to oxcitons, schematically shown in Fig. 2(c).

These spectroscopic signatures are also observed in complementary magneto-absorption studies of another charge-tunable ML-WSe₂, shown in Fig. 2. Here, n_e is fixed and B is swept from 0-55 T in a pulsed magnet (see Ref. [25] for sample and experimental details). When n_e is set just below the point where electrons begin to fill the top CB valleys (at zero field), then the combination of valley Zeeman splitting and LL formation forces the upper CB in K to repeatedly fill and empty as B increases. Figure 2(b) shows the calculated chemical po-

tential of the Fermi sea (black solid line), superimposed on the LL fan diagram. Repeated Pauli blocking and unblocking of the resonance in K is observed. Concomitantly, the resonance in $-K$ exhibits an abrupt redshift of ~ 3 meV whenever electrons occupy the third CB valley, indicating an abrupt increase in the binding energy of the excitonic state. As with the gate-dependent studies in Figs. 1(c) and (d), this behavior is consistent with the hexciton-to-oxciton transition, occurring when the number of distinguishable electron reservoirs (with which the photoexcited e-h pair in $-K$ can interact) increases from two to three.

We emphasize that the observed discontinuities of the resonance as a function of n_e and B cannot be explained within a picture of transitions between free-particle LLs in the CB and VB, and are not consistent with our own previous claim for coupling between excitons and intervalley plasmons [46, 47]. The Supplementary Material (SM) provides further evidence against the possibilities that neither intervalley plasmons nor optical transitions between LLs of free electron-hole pairs can stand behind the observed phenomena.

A third spectroscopic feature supporting hexcitons is the LL separation $\hbar\omega_c = \hbar eB/m^*$, where ω_c is the cyclotron frequency and m^* is the effective mass. As indicated by the arrows in Fig. 1(c), the LL separation increases with gate voltage, revealing that m^* falls from $\sim 0.32m_0$ to $\sim 0.26m_0$ as n_e increases (m_0 is the free-electron mass). These masses are evidently larger than the reduced mass of neutral excitons in WSe₂ [48, 49], and are much closer to the electron mass in the top CB valleys [50]. Thus, the LLs are likely related to the quantized motion of the top-valley electron. We explain how this behavior, and also the redshift of the LLs with increasing n_e , are consistent with optical transitions of hexcitons.

Figure 3 shows calculated average inter-particle distances within the hexciton as a function of the electron density. Details of the theory needed for these calculations are presented in Refs. [40, 41], and here we discuss the results in the experimental context. r_{he} is the calculated average distance between the VB hole and electron in the bottommost CB valley. r_{ee} denotes the respective distance between the two electrons in the bottommost CB valley. Compared with the other shown cases, the small values of r_{he} and r_{ee} imply that the trion at the hexciton core is dark, comprising the optically inactive bottom-valley electrons. The VB hole prefers binding tightly to these two electrons on accounts of their heavier mass compared with that of the photoexcited electron in the top valley [49–51]. As depicted in Fig. 3(c), the latter behaves as a ‘satellite’, capturing the electron-depleted region around the core trion, rendered by the two CB holes. As evident from the distance between the satellite electron and the VB hole (r_{ht}), the binding of the former to the complex is relatively weak at small electron

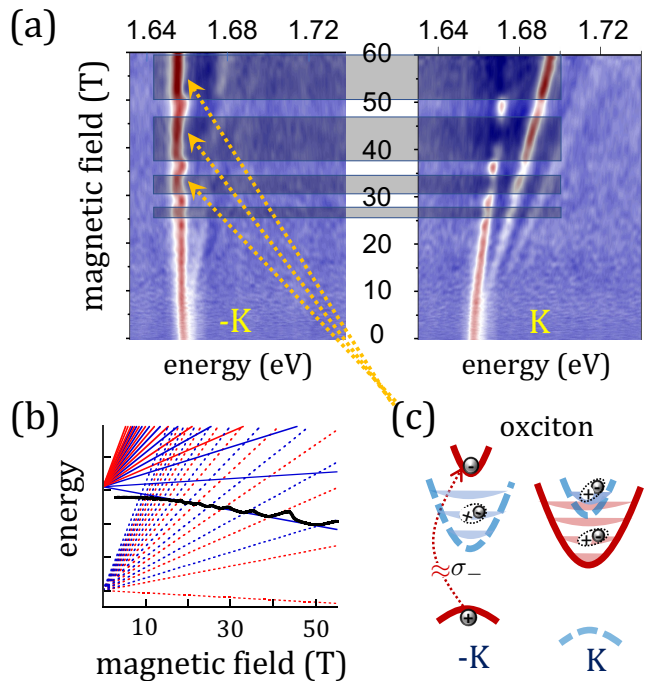


FIG. 2. (a) Magneto-optical reflectance spectra as a function of magnetic field and photon energy in a second device. The voltage level is at the threshold of filling the top CB valley of K . The shaded boxes show the regimes at which the top valley at K is filled. (b) Spin- and valley-resolved LL diagrams in the CBs within a single-electron picture. The solid black line denotes the chemical potential of the Fermi sea. (c) The exciton state, formed when the trion at its core binds to three Fermi holes in the CB and two satellite electrons. The hexciton-to-oxciton transition takes place when the top CB valley at K has one filled Landau level, marked by the shaded regions in (a).

densities, as shown by the inset of Fig. 3. The spatial extent of the CB holes is large at small densities, as can be understood from the average distances between the VB and CB holes ($r_{h\bar{e}}$) or between the CB holes ($r_{\bar{e}\bar{e}}$). Connecting these results with the experimental findings, the effective mass we extract from the energy difference between LLs in Figs. 1(c) and (d) is nearly that of a top-valley free electron at small electron densities (i.e., when its binding to the complex is small). The energy difference between LLs increases when the density increases, indicating of a smaller effective mass. This behavior implies that the motion of the satellite electron and core dark trion becomes correlated, caused by tighter binding of the former to the hexciton, as shown in Fig. 3. The effective mass in this case would ultimately correspond to the reduced mass, $1/m^* = 1/m_t + 1/M_D$ where M_D is the translational mass of the dark trion ($M_D \sim 4m_t$ in ML WSe₂ [51]).

Additional support for the presence of hexcitons can be found in the photoluminescence (PL) spectrum. Figure 4 shows the low-temperature PL intensity at zero

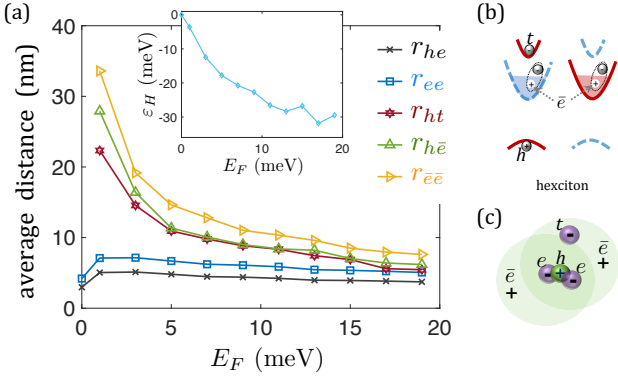


FIG. 3. (a) Calculated inter-particle distances in the hexciton as a function of the Fermi energy ($E_F \approx 5$ meV amounts to $n = 10^{12} \text{ cm}^{-2}$). (a) Results are shown for average distances between the CB electron and VB hole (r_{he}), between the two CB electrons of the core trion (r_{ee}), between the VB hole and the outer top-valley electron (r_{ht}) or CB holes ($r_{h\bar{e}}$), and between the CB holes ($r_{e\bar{e}}$). Inset: Calculated binding energy of the satellite electron to the hexciton. (b) and (c) Schemes of the hexciton in k -space and real-space, respectively. The trion at the core of the hexciton binds to two CB holes and a satellite electron.

magnetic field from a third-charge tunable ML-WSe₂ device. Optical transitions of this device close to charge neutrality were analyzed in Ref. [52]. Here, we focus on the dominant transition when the ML is electron rich, marked with H (hereafter we refer to $X^{-'}$ as H). Its PL intensity is noticeable when the gate voltage is larger than ~ 2 V. If the hexciton picture is correct, then the energy of the peak H should emerge from $\hbar\omega_{D^-} + \Delta_c$ at small electron densities, where $\hbar\omega_{D^-}$ is the optical-transition energy of the dark trion and $\Delta_c \simeq 14$ meV is the spin splitting energy between the bottom and top CB valleys [53]. To understand this reasoning, we recall that the binding energy of the hexciton is that of the dark trion at its core when the spatial extent of the CB holes is large (small density), which in turn means that the outer (top-valley) electron is loosely bound to the complex. Yet, the energy emerges from $\hbar\omega_{D^-} + \Delta_c$ rather than $\hbar\omega_{D^-}$ because the optical transition involves the tightly bound VB hole and loosely bound top-valley electron. When the electron density increases, the spatial extent of the CB holes shrinks and the binding of the outer electron to the complex increases, as shown in Fig. 3. Hence the observed redshift and amplified PL.

We explain the observed behavior in Fig. 4 as follows. Hexcitons correspond to three optical transitions marked with H , D^- and D_B^- when the electron density is large. Each of these transitions correspond to the recombination of a different electron in the complex with the VB hole. At small electron densities, shown by the voltage range $\lesssim 2$ V in Fig. 4(a), the outer top-valley electron is still far from the complex, resulting in vanishing PL intensity of the peak H . Despite having ‘wrong’ quan-

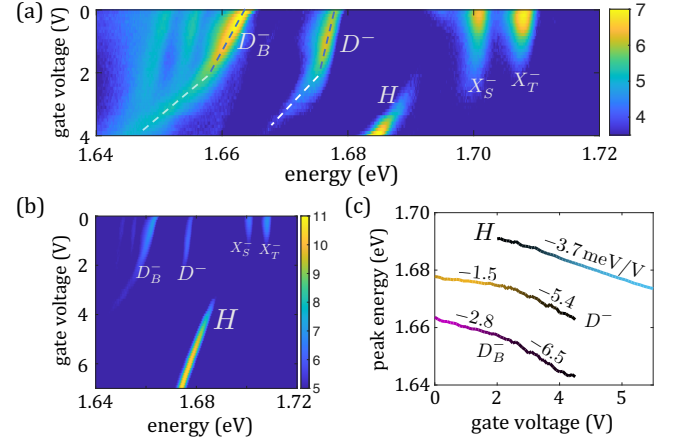


FIG. 4. (a) Log-scale colormap of the photoluminescence intensity in electron-doped ML-WSe₂ at 4 K. The hexciton peak, marked with H (often dubbed $X^{-'}$ in the literature), emerges around 2 V. The secondary transitions emerge from the dark trion optical transitions, D^- and D_B^- (see text), and their redshift is enhanced when the peak H emerges. (b) The colormap in a larger voltage range, showing the dominance of H in the electron-rich regime. (c) Peak energies of H , D^- and D_B^- . The line brightness denotes the normalized PL intensity of the peak and the redshift numbers are in meV per Volt.

tum numbers, the PL intensities of the dark trion and its brightened component are stronger than H when the electron density is small: D^- (D_B^-) involves recombination of the electron with opposite spin (valley) compared to that of the missing electron in the VB. The peak H emerges gradually when the electron density continues to increase; a result of the tighter binding of the top-valley electron to the hexciton. With the emergence of H , the redshifts of D^- and D_B^- are enhanced, accompanied with their gradual decay. Figure 4(c) shows the peak energies of H , D^- and D_B^- , where the brightness of the line corresponds to the normalized PL intensity of the peak. The redshifts of D^- and D_B^- are enhanced around ~ 2 V, where the slope of D^- changes from -1.5 to -5.4 meV/V, and that of D_B^- from -2.8 to -6.5 meV/V. The differences match nearly perfectly with the slope of H (-3.7 meV/V). The density regime at which the slopes of D^- and D_B^- are enhanced mark the transition from trions to hexcitons. Consistent with that, the emergence of H in Fig. 4(a) is also accompanied with fading of the bright trions ($X_{S,T}^-$). The SM includes further analysis on the redshifts of H , D^- and D_B^- .

In conclusion, we have provided supporting evidence for the presence of hexcitons and excitons in electron rich ML-WSe₂. While this achievement is important on its own merits, lest we lose sight of the wider implications. Among the various mechanisms proposed in the literature so far to explain optical transitions of bound excitonic states in doped semiconductors, our findings reinforce the viability of composite excitonic states [40, 41].

The unique band structure of ML-WSe₂ allows us not only to reinforce this idea but to provide the following general principle. When the exciton binding energy of the semiconductor exceeds the Fermi energy, bound excitonic states are made of one or more electron-hole pairs, where the hole of at least one pair is from the VB. Other electron-hole pairs are made of CB holes and electrons with distinct spin-valley configuration. The possible number of pairs in a composite excitonic state is determined by the spin-valley space at the edge of the CB (or VB by reversing the discussion to *p*-type doping).

In experiment, composite excitonic states are seen when the charge density is such that the spatial extent of CB holes is not far larger than the bare-trion radius. In this regime, CB holes can further glue extra electrons around the core trion. Many semiconductors, including zinc blende compounds, can host up to two electrons in a tetron-type configuration [42]. Other semiconductors can host larger composites, such as the hexciton or oxciton in ML-WSe₂, and possibly beyond that in multi-valley semiconductors. The observation of such many-body correlated complexes can be facilitated by engineering the dielectric environment to enhance the binding energies. Using magnetic fields or strain to lift the spin and valley (pseudospin) degeneracies, one can further control the size of the excitonic state.

Dinh Van Tuan is supported by the Department of Energy, Basic Energy Sciences, Division of Materials Sciences and Engineering under Award DE-SC0014349. Hanan Dery is supported by the Office of Naval Research, under Award N000142112448. The work at NHMFL (Scott A. Crooker) is supported by NSF DMR-1644779, the State of Florida, and the Department of Energy. Xiaodong Xu is supported by Department of Energy, Basic Energy Sciences, under award DE-SC0018171. Su-Fei Shi is supported by NSF, under Career award DMR-1945420 and award DMR-2104902.

* hanan.dery@rochester.edu

- [1] R. J. Elliott, Intensity of optical absorption by excitons, *Phys. Rev.* **108**, 1384 (1957).
- [2] L. D. Laude, F. H. Pollak, and M. Cardona, Effects of uniaxial stress on the indirect exciton spectrum of silicon, *Phys. Rev. B* **3**, 2623 (1971).
- [3] Excitons (Modern Problems in Condensed Matter Sciences) Ed. E. I. Rashba and M. D. Sturge, (Elsevier, 1987).
- [4] H. Haug and S. W. Koch, Quantum theory of the optical and electronic properties of semiconductors, 3rd ed. (World Scientific, Singapore, 1994).
- [5] M. Combescot and S.-Y. Shiau, Excitons and Cooper pairs: two composite bosons in many-body physics, (Oxford University Press, Singapore, 2016).
- [6] G. D. Mahan, Excitons in degenerate semiconductors, *Phys. Rev.* **153**, 882 (1967).
- [7] H. Haug and S. Schmitt-Rink, Electron theory of the optical properties of laser excited semiconductors, *Prog. Quant. Electr.* **9**, 3 (1984).
- [8] Y.-C. Chang and G. D. Sanders, Band-mixing effect on the emission spectrum of modulation-doped semiconductor quantum wells, *Phys. Rev. B* **32**, 5521(R) (1985).
- [9] R. Sooryakumar, A. Pinczuk, A. C. Gossard, D. S. Chemla, and L. J. Sham, Tuning of the valence-band structure of GaAs quantum wells by uniaxial stress, *Phys. Rev. Lett.* **58**, 1150 (1987).
- [10] M. S. Skolnick, J. M. Rorison, K. J. Nash, D. J. Mowbray, P. R. Tapster, S. J. Bass, and A. D. Pitt, Observation of a many-body edge singularity in quantum-well luminescence spectra, *Phys. Rev. Lett.* **58**, 2130 (1987).
- [11] P. Hawrylak, Optical properties of a two-dimensional electron gas: evolution of spectra from excitons to fermi-edge singularities, *Phys. Rev. B* **44**, 3821 (1991).
- [12] C. L. Kane, K. A. Matveev, and L. I. Glazman, Fermi-edge singularities and backscattering in a weakly interacting one-dimensional electron gas, *Phys. Rev. B* **49**, 2253 (1994).
- [13] K. Kheng, R. T. Cox, Merle Y. d'Aubigné, F. Bassani, K. Saminadayar, and S. Tatarenko, Observation of negatively charged excitons X^- in semiconductor quantum wells, *Phys. Rev. Lett.* **71**, 1752 (1993).
- [14] B. Stébé and A. Ainane, Ground state energy and optical absorption of excitonic trions in two dimensional semiconductors, *Superlattices microstruct.* **5**, 545 (1989).
- [15] G. Finkelstein, H. Shtrikman, and I. Bar-Joseph, Optical spectroscopy of a two-dimensional electron gas near the metal-insulator transition, *Phys. Rev. Lett.* **74**, 976 (1995).
- [16] G. V. Astakhov, V. P. Kochereshko, D. R. Yakovlev, W. Ossau, J. Nurnberger, W. Faschinger, and G. Landwehr, Oscillator strength of trion states in ZnSe-based quantum wells, *Phys. Rev. B* **62**, 10345 (2000).
- [17] A. S. Bracker, E. A. Stinaff, D. Gammon, M. E. Ware, J. G. Tischler, D. Park, D. Gershoni, A. V. Filinov, M. Bonitz, F. Peeters, and C. Riva, Binding energies of positive and negative trions: From quantum wells to quantum dots, *Phys. Rev. B* **72**, 035332 (2005).
- [18] V. Huard, R. T. Cox, K. Saminadayar, A. Arnoult, and S. Tatarenko, Bound states in optical absorption of semiconductor quantum wells containing a two-dimensional electron gas, *Phys. Rev. Lett.* **84**, 187 (2000).
- [19] G. Wang, A. Chernikov, M. M. Glazov, T. F. Heinz, X. Marie, T. Amand, and B. Urbaszek, Colloquium: Excitons in atomically thin transition metal dichalcogenides, *Rev. Mod. Phys.* **90**, 021001 (2018).
- [20] Z. Wang, L. Zhao, K. F. Mak, and J. Shan, Probing the spin-polarized electronic band structure in monolayer transition metal dichalcogenides by optical spectroscopy, *Nano Lett.* **17**, 740 (2017).
- [21] T. Smoleński, O. Cotlet, A. Popert, P. Back, Y. Shimazaki, P. Knüppel, N. Dietler, T. Taniguchi, K. Watanabe, M. Kroner, and A. Imamoglu, Interaction-induced Shubnikov-de Haas oscillations in optical conductivity of monolayer MoSe₂, *Phys. Rev. Lett.* **123**, 097403 (2019).
- [22] T. Wang, Z. Li, Z. Lu, Y. Li, S. Miao, Z. Lian, Y. Meng, M. Blei, T. Taniguchi, K. Watanabe, S. Tongay, W. Yao, D. Smirnov, C. Zhang, and S.-F. Shi, Observation of quantized exciton energies in monolayer WSe₂ under a strong magnetic field, *Phys. Rev. X* **10**, 021024 (2020).
- [23] E. Liu, J. van Baren, T. Taniguchi, K. Watanabe, Y.-

- C. Chang, and C. H. Lui, Landau-quantized excitonic absorption and luminescence in a monolayer valley semiconductor, *Phys. Rev. Lett.* **124**, 097401 (2020).
- [24] E. Liu, J. van Baren, Z. Lu, T. Taniguchi, K. Watanabe, D. Smirnov, Y.-C. Chang, and C.-H. Lui, Exciton-polaron Rydberg states in monolayer MoSe₂ and WSe₂, *Nat. Commun.* **12**, 6131 (2021).
- [25] J. Li, M. Goryca, J. Choi, X. Xu, S. A. Crooker, Many-body exciton and intervalley correlations in heavily electron-doped WSe₂ monolayers, *Nano Lett.* **22**, 426 (2022).
- [26] R. Schmidt, M. Knap, D. A. Ivanov, J.-S. You, M. Cetina, and E. Demler, Universal many-body response of heavy impurities coupled to a Fermi sea: a review of recent progress, *Rep. Prog. Phys.* **81**, 024401 (2018).
- [27] P. Massignan, M. Zaccanti, and G. M. Bruun, Polarons, dressed molecules and itinerant ferromagnetism in ultracold Fermi gases, *Rep. Prog. Phys.* **77**, 034401 (2014).
- [28] M. Sidler, P. Back, O. Cotlet, A. Srivastava, T. Fink, M. Kroner, E. Demler, and A. Imamoglu, Fermi polaron-polaritons in charge-tunable atomically thin semiconductors, *Nat. Phys.* **13**, 255 (2017).
- [29] D. K. Efimkin and A. H. MacDonald, Many-body theory of trion absorption features in two-dimensional semiconductors, *Phys. Rev. B* **95**, 035417 (2017).
- [30] D. K. Efimkin and A. H. MacDonald, Exciton-polarons in doped semiconductors in a strong magnetic field, *Phys. Rev. B* **97**, 235432 (2018).
- [31] C. Fey, P. Schmelcher, A. Imamoglu, and R. Schmidt, Theory of exciton-electron scattering in atomically thin semiconductors, *Phys. Rev. B* **101**, 195417 (2020).
- [32] R. A. Suris, V. P. Kochereshko, G. V. Astakhov, D. R. Yakovlev, W. Ossau, J. Nurnberger, W. Faschinger, G. Landwehr, T. Wojtowicz, G. Karczewski, and J. Kossut, Excitons and trions modified by interaction with a two-dimensional electron gas, *Phys. Stat. Sol. (b)* **227**, 343 (2001).
- [33] A. Esser, R. Zimmermann, and E. Runge, Theory of trion spectra in semiconductor nanostructures, *Phys. Stat. Sol. (b)* **227**, 317 (2001).
- [34] F. X. Bronold, Absorption spectrum of a weakly *n*-doped semiconductor quantum well, *Phys. Rev. B* **61**, 12620 (2000).
- [35] V. Koudinov, C. Kehl, A. V. Rodina, J. Geurts, D. Wolverson, and G. Karczewski, Suris Tetrons: Possible spectroscopic evidence for four-particle optical excitations of a two-dimensional electron gas, *Phys. Rev. Lett.* **112**, 147402 (2014).
- [36] F. Rana, O. Koksai, and C. Manolatu, Many-body theory of the optical conductivity of excitons and trions in two-dimensional materials, *Phys. Rev. B* **102**, 085304 (2020).
- [37] Y.-C. Chang, S.-Y. Shiau, and M. Combescot, Crossover from trion-hole complex to exciton-polaron in *n*-doped two-dimensional semiconductor quantum wells, *Phys. Rev. B* **98**, 235203 (2018).
- [38] M. M. Glazov, Optical properties of charged excitons in two-dimensional semiconductors, *J. Chem. Phys.* **153**, 034703 (2020).
- [39] D. K. Efimkin, E. K. Laird, J. Levinsen, M. M. Parish, and A. H. MacDonald, Electron-exciton interactions in the exciton-polaron problem, *Phys. Rev. B* **103**, 075417 (2021).
- [40] D. Van Tuan and H. Dery, Composite excitonic states in doped semiconductors, arXiv:2202.08374.
- [41] D. Van Tuan and H. Dery, Turning many-body problems to few-body ones in photoexcited semiconductors using the stochastic variational method in momentum space, SVM-*k*, arXiv:2202.08378.
- [42] D. Van Tuan and H. Dery, Tetrons, pexcitons, and hexcitons in monolayer transition-metal dichalcogenides, arXiv:2202.08379.
- [43] A. M. Jones, H. Yu, J. Schaibley, J. Yan, D. G. Mandrus, T. Taniguchi, K. Watanabe, H. Dery, W. Yao, and X. Xu, Excitonic luminescence upconversion in a two-dimensional semiconductor, *Nat. Phys.* **12**, 323 (2016).
- [44] E. Courtade, M. Semina, M. Manca, M. M. Glazov, C. Robert, F. Cadiz, G. Wang, T. Taniguchi, K. Watanabe, M. Pierre, W. Escoffier, E. L. Ivchenko, P. Renucci, X. Marie, T. Amand, and B. Urbaszek, Charged excitons in monolayer WSe₂: experiment and theory, *Phys. Rev. B* **96**, 085302 (2017).
- [45] A. M. Jones, H. Yu, N. J. Ghimire, S. Wu, G. Aivazian, J. S. Ross, B. Zhao, J. Yan, D. G. Mandrus, D. Xiao, W. Yao, and X. Xu, Optical generation of excitonic valley coherence in monolayer WSe₂, *Nat. Nano.* **8**, 634 (2013).
- [46] H. Dery, Theory of intervalley Coulomb interactions in monolayer transition-metal dichalcogenides, *Phys. Rev. B* **94**, 075421 (2016).
- [47] D. Van Tuan, B. Scharf, I. Žutić, H. Dery, Marrying excitons and plasmons in monolayer transition-metal dichalcogenides, *Phys. Rev. X* **7**, 041040 (2017).
- [48] A. V. Stier, N. P. Wilson, K. A. Velizhanin, J. Kono, X. Xu, and S. A. Crooker, Magneto-optics of exciton Rydberg states in a monolayer semiconductor, *Phys. Rev. Lett.* **120**, 057405 (2018).
- [49] D. Van Tuan, M. Yang, and H. Dery, Coulomb interaction in monolayer transition-metal dichalcogenides, *Phys. Rev. B* **98**, 125308 (2018).
- [50] A. Kormányos, G. Burkard, M. Gmitra, J. Fabian, V. Zolyomi, N. D. Drummond, and V. Fal'ko, *k* · *p* theory for two-dimensional transition metal dichalcogenide semiconductors, *2D Mater.* **2**, 022001 (2015).
- [51] M. Yang, L. Ren, C. Robert, D. V. Tuan, L. Lombez, B. Urbaszek, X. Marie, and H. Dery, Relaxation and darkening of excitonic complexes in electrostatically-doped monolayer semiconductors: Roles of exciton-electron and trion-electron interactions, *Phys. Rev. B* **105**, 085302 (2022).
- [52] M. He, P. Rivera, D. V. Tuan, N. P. Wilson, M. Yang, T. Taniguchi, K. Watanabe, J. Yan, D. G. Mandrus, H. Yu, H. Dery, W. Yao, and X. Xu, Valley phonons and exciton complexes in a monolayer semiconductor, *Nat. Commun.* **11**, 618 (2020).
- [53] P. Kapuściński, A. Delhomme, D. Vaclavkova, A. O. Slobodeniuk, M. Grzeszczyk, M. Bartos, K. Watanabe, T. Taniguchi, C. Faugeras, and M. Potemski, Rydberg series of dark excitons and the conduction band spin-orbit splitting in monolayer WSe₂, *Commun. Phys.* **4**, 186 (2021).
- [54] See Supplemental Material at <http://link.aps.org/supplemental...> for details on the optical transitions H , D^- , and D_B^- , as well as further support to rule out the possibility that intervalley plasmons or free electron-hole optical transitions are behind the observed phenomena. The Supplemental Material includes Refs. [55]–[63].
- [55] E. Liu, J. van Baren, C.-T. Liang, T. Taniguchi, K. Watanabe, N. M. Gabor, Y.-C. Chang, and C.-H. Lui,

- Multipath optical recombination of intervalley dark excitons and trions in monolayer WSe₂, *Phys. Rev. Lett.* **124**, 196802 (2020).
- [56] J. P. Echeverry, B. Urbaszek, T. Amand, X. Marie, and I. C. Gerber, Splitting between bright and dark excitons in transition metal dichalcogenide monolayers, *Phys. Rev. B* **93**, 121107(R) (2016).
 - [57] K. Kośmider, J. W. González, and J. Fernández-Rossier, Large spin splitting in the conduction band of transition metal dichalcogenide monolayers, *Phys. Rev. B* **88**, 245436 (2013).
 - [58] H. Dery and Y. Song, Polarization analysis of excitons in monolayer and bilayer transition-metal dichalcogenides, *Phys. Rev. B* **92**, 125431 (2015).
 - [59] Y. Song and H. Dery, Transport theory of monolayer transition-metal dichalcogenides through symmetry, *Phys. Rev. Lett.* **111**, 026601 (2013).
 - [60] C. Robert, H. Dery, L. Ren, D. Van Tuan, E. Courtade, M. Yang, B. Urbaszek, D. Lagarde, K. Watanabe, T. Taniguchi, T. Amand, and X. Marie, Measurement of conduction and valence bands *g*-factors in a transition metal dichalcogenide monolayer, *Phys. Rev. Lett.* **126**, 067403 (2021).
 - [61] A. O. Slobodeniuk and D. M. Basko, Spin-flip processes and radiative decay of dark intravalley excitons in transition metal dichalcogenide monolayers, *2D Mater.* **3**, 035009 (2016).
 - [62] M. Danovich, V. Zolyomi, and V. I. Fal'ko, Dark trions and biexcitons in WS₂ and WSe₂ made bright by e-e scattering, *Sci. Rep.* **7**, 45998 (2017).
 - [63] J.-S. Tu, S. Borghardt, D. Grützmacher, and B. E. Kardynal, Experimental observation of a negative grey trion in an electron-rich WSe₂ monolayer, *J. Phys.: Condens. Matter* **31**, 415701 (2019).